A CHEMICAL, THERMOGRAVIMETRIC AND X-RAY STUDY OF CANCRINITE

by

SHU-MEEI CHEN, B. Sc.

A Thesis

Submitted to the School of Graduate Studies

in Partial Fulfilment of the Requirements

for the Degree

Master of Science

McMaster University

September, 1970

STUDIES ON CANCRINITE

MASTER OF SCIENCE
(Geology)

McMASTER UNIVERSITY
Hamilton, Ontario.

TITLE: A Chemical, Thermogravimetric and X-Ray Study of Cancrinite.

AUTHOR: Shu-Meei Chen, B. Sc. (National Taiwan University)

SUPERVISOR: Professor B. J. Burley

NUMBER OF PAGES: 65, viii.

SCOPE AND CONTENTS: Four specimens of natural cancrinite from Ontario were studied. Single crystal photographs were taken and non-Bragg reflections were observed. Changes in these reflections in samples heated to 410°, 600°, and 745°C were investigated. Phase changes in these heated cancrinites were also studied. Suggestions have been made as to the origin of the non-Bragg reflections.

ACKNOWLEDGEMENTS

The writer wishes to express her sincere appreciation to Professor B. J. Burley, her supervisor, for many discussions and corrections of the manuscript.

Thanks are also extended to Dr. H. D. Grundy for his help with taking precession photographs, to J. Muysson, who did the chemical analyses and to F. Tebay, who took care of the x-ray equipment.

Financial support was provided by the Department of Geology, McMaster University, the National Research Council and the Geological Survey of Canada.

TABLE OF CONTENTS

LIST OF TABLES

LIST OF FIGURES

LIST OF PLATES

ABSTRACT

Cancrinite specimens from Ontario were studied. Chemical and Thermogravimetric analyses were made. Non-Bragg reflections were observed in x-ray photographs. These reflections have the same symmetry as the main lattice reflections, but the intensities, abundance and the relative positions of them with respect to the main lattice reflections are different from one specimen to another. In the heated specimens, the superstructure reflections decrease in intensities, shift in position and are streaked in a direction parallel to the a^*-axis on the $a^* c^*$ reciprocal lattice plane.

Phase changes in the heated cancrinites show that the sodalite group of minerals occur as transitional phases in the cancrinite break down reactions.

It is shown that the non-Bragg reflections are very similar to the main lattice reflections. There is a probable relation between the non-Bragg reflections in cancrinite and the sodalite group of minerals.

CHAPTER 1
INTRODUCTION

Four specimens of natural cancrinite from Ontario were studied. Precession photographs were taken for each specimen. All of the photographs show superstructure reflections. Trying to eliminate these extra reflections, the specimens were heated to various temperatures to see how these superstructure reflections change with temperature. In order to choose suitable temperatures to which cancrinite was to be heated, a thermogravimetric analysis was made.

The detailed structure of cancrinite is not yet known. Many previous workers have attempted the structure of cancrinite by ignoring the superstructure reflections. In single crystal pictures of heated cancrinites, significant changes in superstructure reflections, e.g. a decrease in intensities and a shifting in position, were observed. This provided evidence on the cause of superstructure reflections. A phase transformation was also observed in heated cancrinites. Different specimens resulted in different transformation products at different temperatures. The transformation products were identified by x-ray powder diffractometry. Some suggestions have been made as to the cause of the differences in transformation temperatures and breakdown products.

Previous works

L. Pauling deduced the davynite-cancrinite framework in 1930. The fundamental unit is the ring of six tetrahedra, also found in sodalite and other silicates. The tetrahedra are alternatively silicon and aluminum tetrahedra, each tetrahedral oxygen being common to one of each kind. The space group of this framework is $P6_3/m\ mc$ (D^4_{6h}). There are cavities in the framework in which the other constituents of the crystals may be placed. It may be seen that there are tunnels along the c-axis in the form of circular cylinders with a diameter of 6 Å (after allowing 3.0 Å for the oxygen ions of the framework). See Fig. 1-1.

Between 1932 and 1933, Kôzu et al. published a series of papers on cancrinite from Dôdô, Korea. They reported its chemical compositions, optical and thermal properties, and crystal structure. A thermobalance was used to study the change in weight of cancrinite during heating. The space group of cancrinite was determined as $P6_3(C^6_6)$. In 1949, Phoenix and Nuffield studied the cancrinite from Blue Mountain, Ontario. Chemical analysis and cell-content were given. Because the sum of Al and Si is greater than 12, based on O = 24, they supposed that some Al substitute for the cations. From analysis of several samples the following general formula was derived.

$$(Na, K, Ca, Al)^{8+-10+}_{6-8}\ Si_6Al_6\ O^{6-}_{24}\ (SO_4, CO_3)^{4^--2^-}_{1-2}\ 1\text{-}5\ H_2O$$

From density and consideration of the electric charge, Phoenix et al.

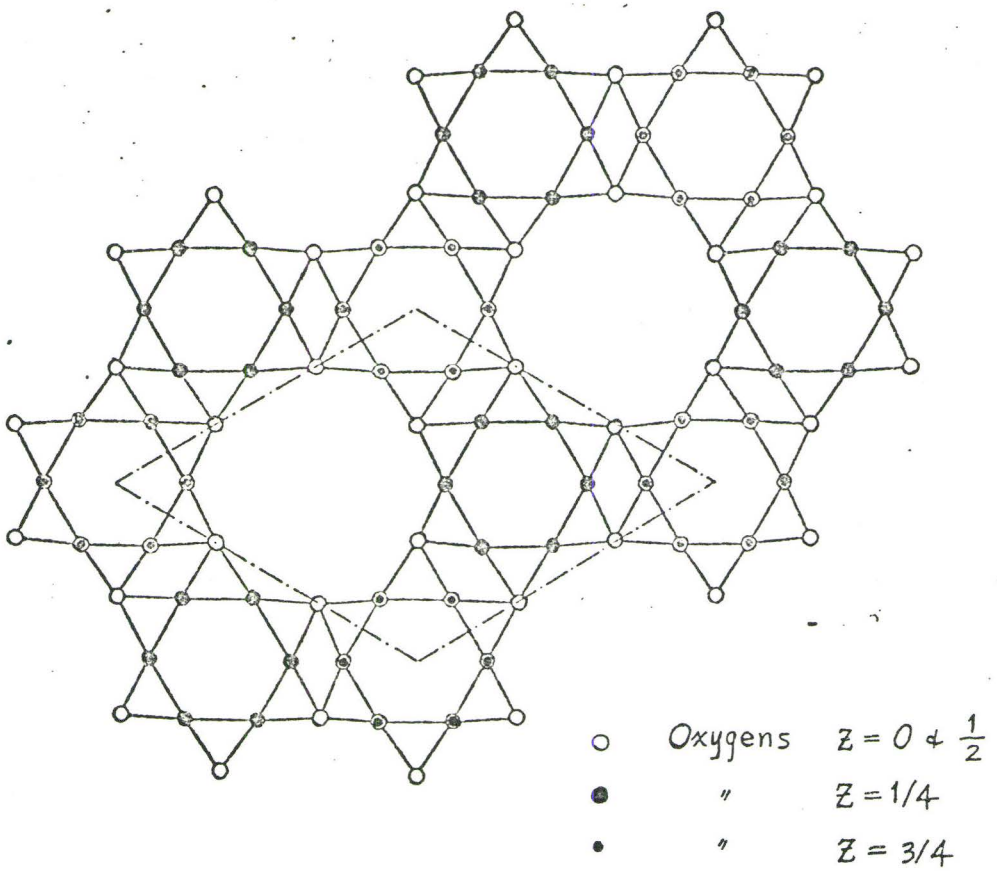

Fig 1-1 The davynite-cancrinite framework projected on (001) (after Pauling)

supposed that cancrinite practically always contains unfilled positions.

P. Nithollon in 1955 determined atomic parameters and interatomic distances of cancrinite from Litchfield (Maine), based on a zeolite structure which consists of rings of six tetrahedra situated around the ternary axes. The H_2O, Ca^{++} and CO_3^{--} occur in the channels formed by these rings.

Edgar and Burley (1963) and Edgar (1964) synthesized various kinds of carbonate, bicarbonate and hydroxyl cancrinites whose stability fields were also investigated. They concluded that there is a wide range of temperature stability of cancrinite minerals depending on their compositions and that the chemistry of cancrinites also affects their breakdown products.

O. Jarchow (1965) examined crystals from Litchfield, Maine and reported that x-ray photographs of (Ca, Na) CO_3 cancrinites show diffuse satellites with indices (h k $l \pm \frac{3}{7}$). The crystal structure was determined from the relationships of the transformation hauyne to cancrinite and refined on three-dimensional data by the least-squares method to R=0.089.

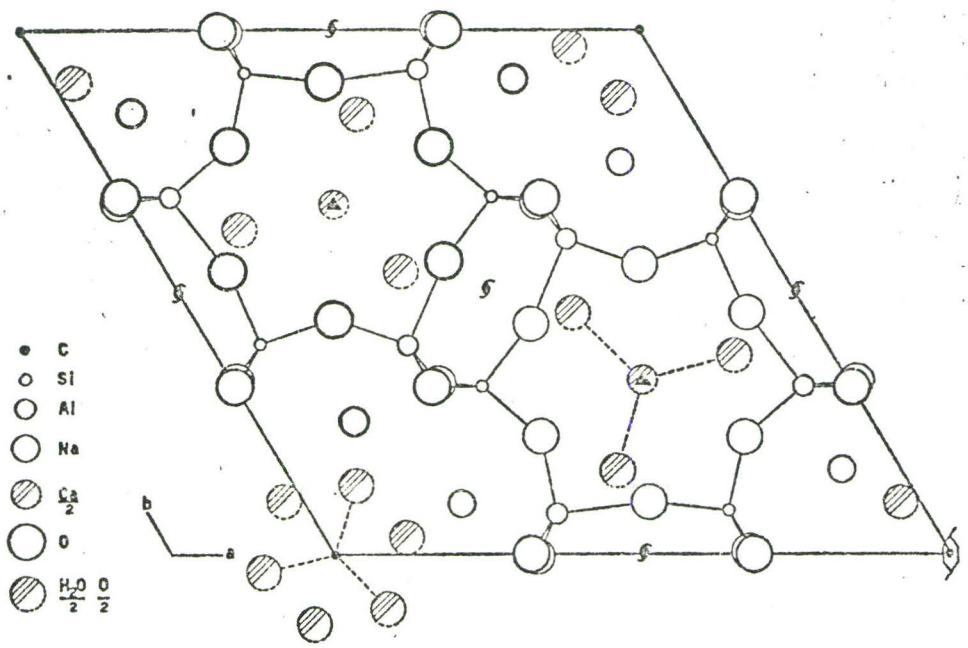

Fig 1-2 Structure of cancrinite, seen along [001], shaded atoms are statistically distributed over the indicated sites, occupying half of these. (after Nithollon)

CHAPTER 2

STUDIES ON PRECESSION PHOTOGRAPHS OF CANCRINITE

2-1 Description of specimens and their chemical analyses

Three out of the four specimens of cancrinite have been analyzed chemically, and the results are listed in Table 2-1. Unfortunately no sulphatic cancrinite was available, those listed in Table 2-1 were common carbonate cancrinites. These specimens are all massive, with perfect prismatic cleavage parallel to $\{10\bar{1}0\}$. They are white or yellow in colour and in thin plates are transparent.

Specimen	Colour	Locality	Remarks
68024	pinkish white	Dungannon Township Ontario	
67001	honey yellow	Blue Mountain Methuen Township Ontario	
67002	white	Dungannon Township Ontario	
6900S	honey yellow	Blue Mountain Methuen Township Ontario	No chemical analysis data

Table 2-1 Chemical Analyses of Cancrinites

oxide \ specimen	68024	67001	67002	1	2
SiO_2	34.35	36.35	33.80	33.98	35.29
Al_2O_3	29.35	29.31	30.65	29.11	28.79
Fe_2O_3					
FeO	.03*	.06*	.04*		
MnO					
MgO	.01	.02	.03		
CaO	8.11	4.99	8.46	4.80	1.49
Na_2O	17.66	17.63	14.01	18.69	15.65
K_2O	.10	.97	.81	.64	4.15
H_2O^+ 110°C	3.02	3.49	3.65	4.34	7.62
H_2O^- 110°C	.11	.49	.78	.23	
CO_2	6.60	5.67	6.05	7.00	1.01
SO_3	.00	.00	.00	1.37	5.76
Cl	.21	.09	.12	.42	
Sum	99.55	99.07	98.40	100.58	100.05
$O \equiv Cl$	.05	.02	.03	.10	
Total	99.50	99.05	98.37	100.48	100.05

*Total Fe as Fe_2O_3

Specimen 1, Cancrinite, Blue Mountain, Ontario, Canada
(Phoenix & Nuffield 1949, Amer. Min., Vol. 34, p. 452)

Specimen 2, Vishnevite, Ilmen Mountains, U.S.S.R
(Zavaritsky 1929) Sulphatic variety.

68024 John Muysson, McMaster University, 1968

67001 " " 1967

67002 " " 1967

Table 2-2 Number of Ions on the Basis of 12 (Si+Al)

Ions	68024	67001	67002	1	2
Si	5.979	6.153	5.801	5.971	6.118
Al	6.021	5.847	6.200	6.032	5.886
Fe	.004	.008	.006		
Mg	.003	.005	.007		
Na	5.959	5.786	4.661	6.368	5.260
Ca	1.512	.905	1.556	.904	.277
K	.023	.210	.177	.144	.919
H_2O^+	1.753	1.970	2.089	2.544	4.408
C	1.569	1.310	1.418	1.679	.239
S				.180	.749
Cl	.062	.025	.035	.125	
Na+K+Ca +Mg+Fe	7.50	6.91	6.41	7.42	6.46
Na+K	5.98	6.00	4.84	6.51	6.18
Ca+Mg+Fe	1.52	0.92	1.57	0.90	0.28
C+S+Cl	1.63	1.34	1.45	1.98	0.99

In Table 2-2, the numbers of ions were recalculated from the chemical analysis data in Table 2-1 on the basis of Si + Al = 12. This usually results in oxygen less than 24. The total numbers of volatiles and cations other than Si and Al were also listed. C+ S + Cl varies between 1.0 and 2.0, Na + K + Ca + Fe + Mg varies between 6.0 and 8.0. We may write down the following chemical formulae:

68024 $(Na_{5.96}Ca_{1.51}K_{0.02})(Al_{6.02}Si_{5.98}O_{23.90})(CO_3)_{1.57}Cl_{0.06}\cdot 1.75H_2O$

67001 $(Na_{5.79}Ca_{0.91}K_{0.21})(Al_{5.85}Si_{6.15}O_{23.67})(CO_3)_{1.31}Cl_{0.03}\cdot 1.97H_2O$

67002 $(Na_{4.66}Ca_{1.56}K_{0.18})(Al_{6.20}Si_{5.80}O_{23.46})(CO_3)_{1.42}Cl_{0.04}\cdot 2.09H_2O$

2-2 Precession photography

Cancrinite crystals about 0.2mm in diameter were selected. Because the cleavage of cancrinite on $\{10\bar{1}0\}$ is perfect, the prism parallel to which the c-axis lies is usually shown. It is necessary to examine the mineral grains under a polarized microscope so that the rational crystallographic directions relative to a mineral grain can be recognized. Also it helps to select well crystallized single crystals without deformation.

The mounting consists of a brass pin to which is attached a small glass fibre, at the end of which the crystal itself is mounted. The cancrinite crystal was mounted so that the hexagonal prism was approximately perpendicular to the glass fibre. After correction of orientation error, the dial axis of the precession camera is coincident with one of the a^* axes, say a_2^* - axis. In this mounting, two sets of reciprocal lattice planes which are 90° apart can be recorded, one is parallel to the $a_1^* a_2^*$ plane, the other is parallel to $a_2^* c^*$ plane, having c and a_1 as precessing axis respectively, as shown in Fig. 2-1

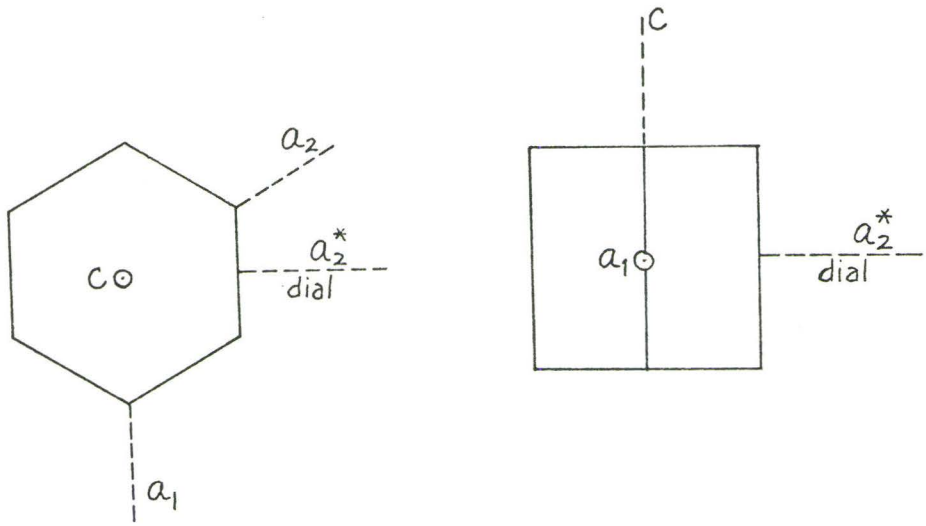

Fig. 2-1 Two settings of cancrinite crystal

2-3 Space group determination.

Precession photographs are especially suitable for space group determination because they are scaled photographs of the reciprocal lattices whose geometrical features carry the space group information. All the qualitative information which can be derived from a set of x-ray diffraction photographs can be concentrated into a short sequence of symbols which together constitute the diffraction symbol. A diffraction symbol is determined by the Friedel symmetry, the lattice type, and the record of the direction of glide planes and screw axes. Such symbols are of great utility in the determination of the space group of a crystal.

Diffraction symbol of cancrinite:

(i) Friedel symmetry:

By inspecting the precession photographs of cancrinite taken for

Table 2-3 Settings of the precession instrument for various layers

a) Reciprocal-lattice planes parallel to $a_1^* a_2^*$

Layer	$\bar{\mu}$	r_s (mm)	$F\lambda d^*$ (mm)	ζ	S (mm)
0	30°	15	0	0	26
1	25°	25	8.34	0.139	30
2	20°	30	16.68	0.278	26.5

b) Reciprocal-lattice planes parallel to $a_2^* c^*$

Layer	$\bar{\mu}$	r_s (mm)	$F\lambda d^*$ (mm)	ζ	S (mm)
0	30°	15	0	0	26
1	25°	20	3.35	0.056	32
2	20°	20	6.70	0.112	29.6
3	20°	25	10.00	0.167	30.3

$\bar{\mu}$: precession angle

r_s: screen radius

F: magnification factor

λ: wavelength of radiation, MoKα was used

S: screen distance

ζ: reciprocal lattice coordinate

various layers, the plane point-group symmetry was determined as follows:

Crystal system	Precessing axis	Lattice level symmetry	
		n-th level	0 level
Hexagonal	$[11\bar{2}0]$	m	2mm
	$[0001]$	6	6

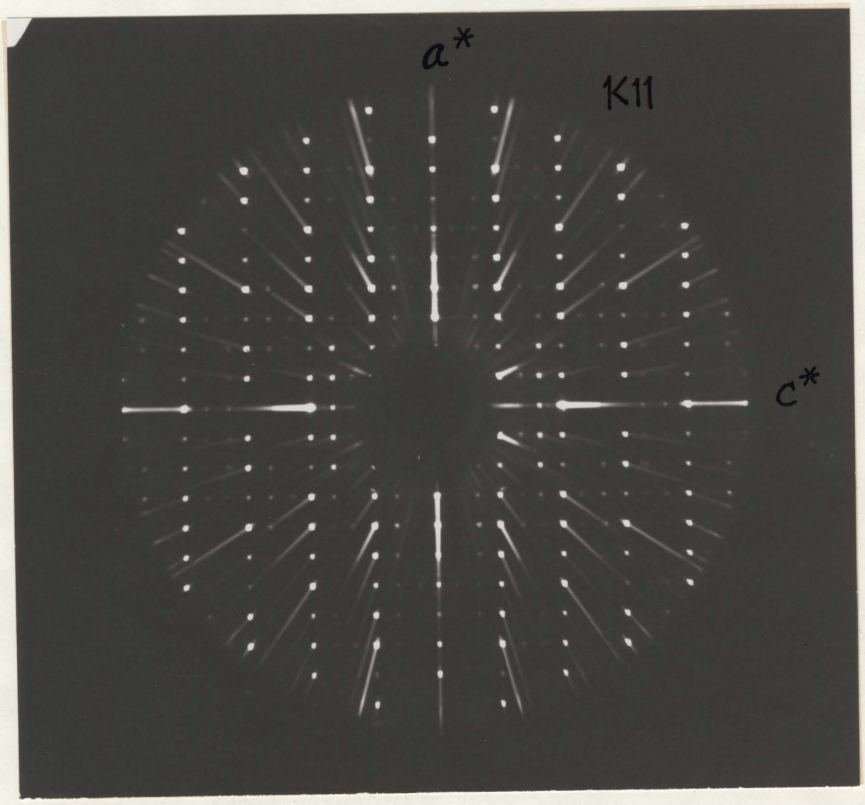

Plate 1 Zero layer precessing axis a, shows 2mm symmetry and three sets of superstructure reflections. (67002,unheated, MoKα,K11).

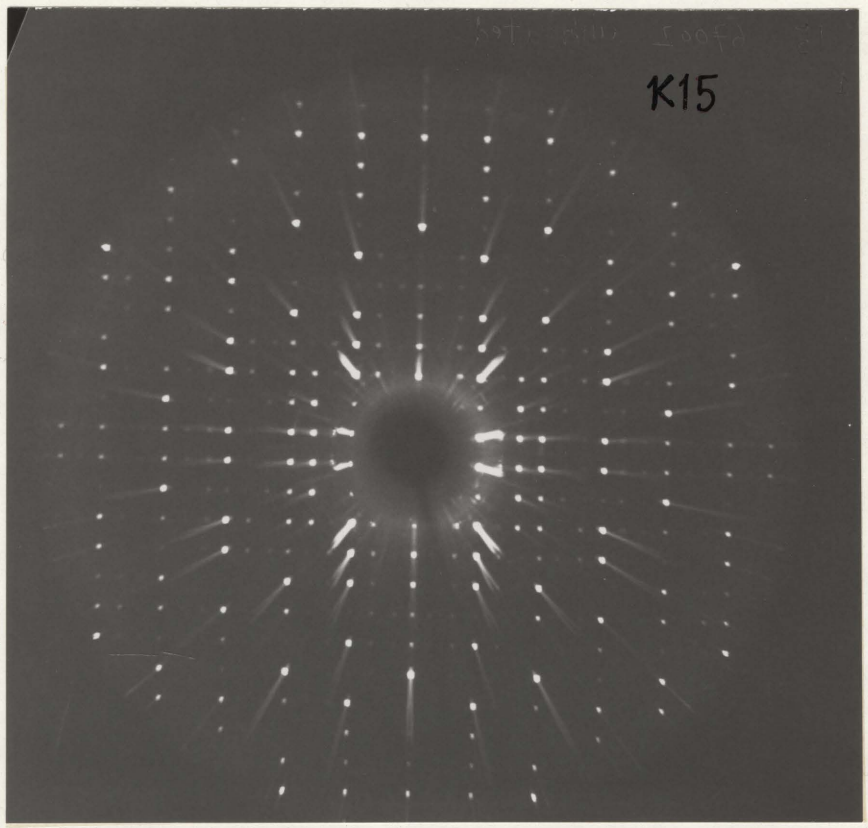

Plate 2 First layer precessing axis a, shows m symmetry (67002, unheated, MoKα, K15).

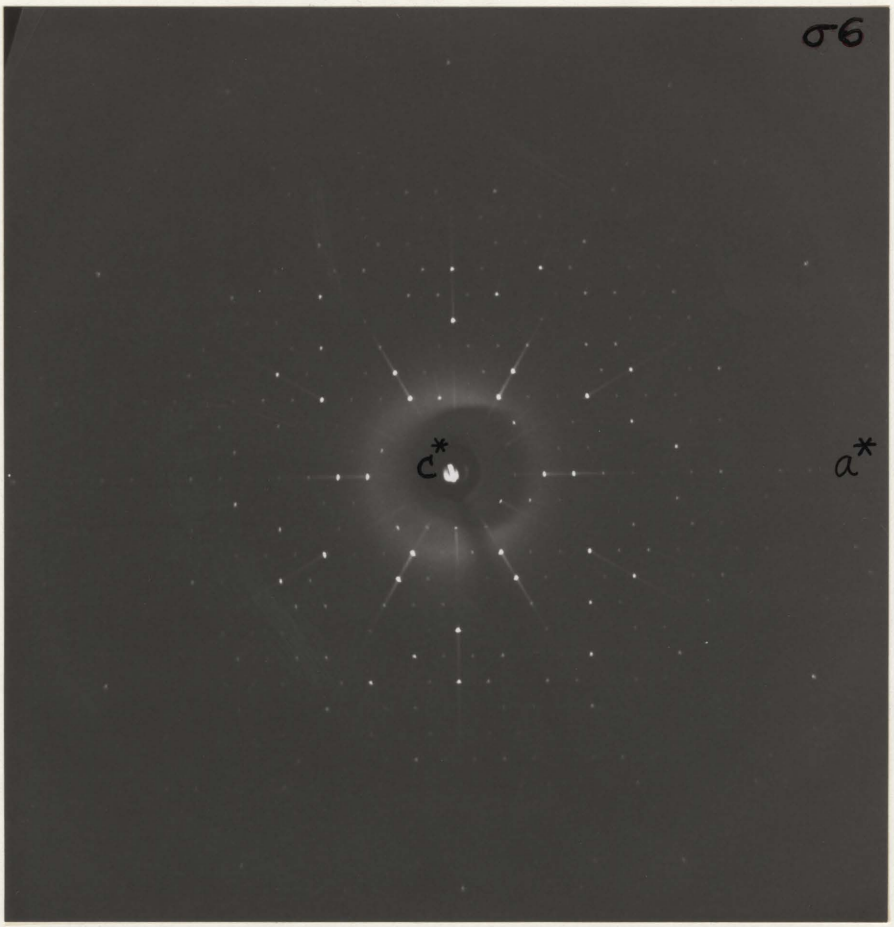

Plate 3 Zero layer precessing axis c, shows 6 symmetry (6900S, unheated MoKα,σ6).

(ii) Lattice type:

If the precession axis and film normal is taken as the a-axis, and on photograph a^* is horizontal, then c^* is vertical where $\gamma^* = 90$. To superimpose the second and third levels in parallel position with the origins coincident, the plane lattices of the two levels not being coincident, displacement must be made along the a^* direction in order to bring the two plane lattices into coincidence.

If the c- axis is taken as the precessing axis, then on the photograph, a_1^* and a_2^* are two sides of a 60^o rhombus, where $\alpha^* = 60^o$. When two adjacent levels are superimposed, the plane lattices of the two levels coincide. So the space lattice of cancrinite is P. When orthogonal axes were used, the alternative unit cell is centered on the C-face.

(iii) Screw axis:

From the pattern of missing reciprocal-lattice points on the zero level photograph , a six-fold screw axis with translation component c/2 was detected. No glide plane was observed, for there is no condition for (0kl) (h0l) and (hk0) reflections.

Plate 1 also shows a 6_3 screw axis for (001) only l=2n reflections are observed

The diffraction symbol and crystal class of cancrinite are $6/mP6_3/-$ and 6 respectively. By consulting Table 34 in X-Ray Crystallography (Buerger) the space group of cancrinite was determined as $P6_3$. (Fig. 2-2).

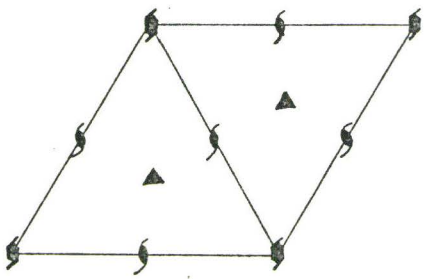

Fig. 2-2 Symmetry of $P6_3$

2-4 Unit cell dimensions

Since precession photographs provide an undistorted picture of the reciprocal lattice, once the reciprocal cell has been measured, the results can be readily transformed into edge lengths and interaxial angles of the direct cell by using standard relations between the two cells.

The reciprocal cell is best measured on a zero-level photograph with a maximum precession angle 30°. For cancrinite, both d^*_{100} and $d^*_{00\bar{1}}$ can be measured on an a-axis precession photograph. A measuring device was used, which can be read by means of a vernier directly to 0.005 cm. The distance between rows of spots parallel to the c^*-axis gives d^*_{100}. A similar procedure is used for obtaining d^*_{001} except the distance between rows parallel to the a^*-axis is required. The interaxial angles between a^* and c^*, and between a_1^* and a_2^* can be measured, which are 90° and 60° respectively. The following is a transformation of edge lengths and interaxial angles of reciprocal cell into those of the direct cell:

$$a = \frac{M\lambda}{d^*_{100}\,\mathrm{Cos}\,30^{\circ}} = \frac{60 \times 0.7107}{3.9 \times 0.866} = 12.63\text{Å}$$

$$c = \frac{M\lambda}{d^*_{001}} = \frac{60 \times 0.7107}{8.3} = 5.13 \text{ Å}$$

$$\gamma = 180^\circ - \gamma^* = 90^\circ$$

$$\alpha = 180^\circ - \alpha^* = 120^\circ$$

in which M and λ are constants, d^*_{100}, d^*_{001}, γ^* and α^* are measured values.

M = 60mm; magnigication factor

λ = 0.7107A; Mo Kα radiation

$d^*_{100} = 3.9$ mm

$d^*_{001} = 8.3$mm

$\gamma^* = a^* c^* = 90^\circ$

$\alpha^* = a_1^* a_2^* = 60^\circ$

The deviation of d^*_{100} and d^*_{001} values measured on precession photographs of the four specimens of cancrinite is within 0.5%. The accuracy of the results is affected by the accuracy of the knowledge of M, the crystal shape and absorption, the centering of the crystal, and the shrinkage of the film.

2-5 Superstructure reflections

On the precession photographs parallel to the $a^* c^*$ reciprocal lattice plane, non-Bragg reflections occur in addition to the normal unit cell reflections. In this thesis, the unit cell reflections with dimensions a_o=12.62Å, C_o=5.13Å will be described as main lattice reflections and the non-Bragg reflections described as superstructure reflections.

In the zero layer containing a^* and c^* axes, the distances between rows of spots parallel to the c^*-axis are the same for the superstructure reflections and the main lattice reflections, in other words, they have the same d^*_{100}

spacing. In the direction perpendicular to the c^* - axis and parallel to the a^* - axis, the superstructure reflections are distributed between the main lattice reflections in such a way that they can be separated into several sets of primitive lattices, each lattice set has the same rectangular unit area as the main structure lattice, except shifting in the direction parallel to the c^* – axis a different amount for each lattice set.

The reciprocal lattices of the superstructure have the same lattice level symmetry and screw axis extinction as the reciprocal lattices of the main structure (see photographs of zero layer and first layer.) but the intensities of the former are much weaker than the latter. The most intense superstructure reflections distribute between (0kl) and (0k2) reflections of the main lattice. Precession photographs of this most intense layer was taken, which shows 6-fold symmetry with 3 principal horizontal axes lying in exactly the same orientation as the 3 axes of the main lattice reflections. (see Plate 7).

Specimens 68024 and 67002 have three sets of superstructure reflections, d, e and f, while specimens 67001 and 6900S just have a prominent set f. Table 2-4 shows the ratio of superstructure (001) spacing to the main lattice (001) spacing. For example, the f set superstructure reflections has a (001) spacing 1.58 times the (001) spacing of the main lattice, 5.125 Å x 1.58 = 8.10Å. Plates 1 and 4 show three sets of superstructure reflections and Plate 5 and 6 show only one set of the superstructure reflections. Plate 7 shows the 6-fold symmetry of the superstructure reflections.

Table 2-4 Ratio of superstructure (001) spacing to the d_{001} of main lattice

Specimen	d	e	f
68024	4.00	2.65	1.58
67001	———	———	1.80
67002	3.47	2.80	1.54
6900S	———	———	1.79

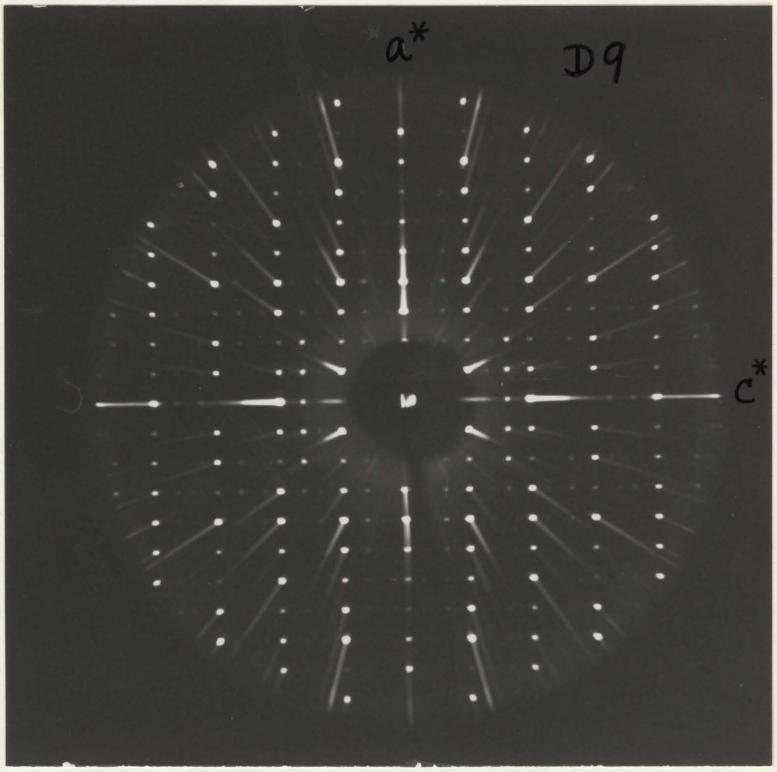

Plate 4 Zero layer of specimen 68024, precessing axis a shows three sets of superstructure reflections.
(68024, unheated MoKα,D9).

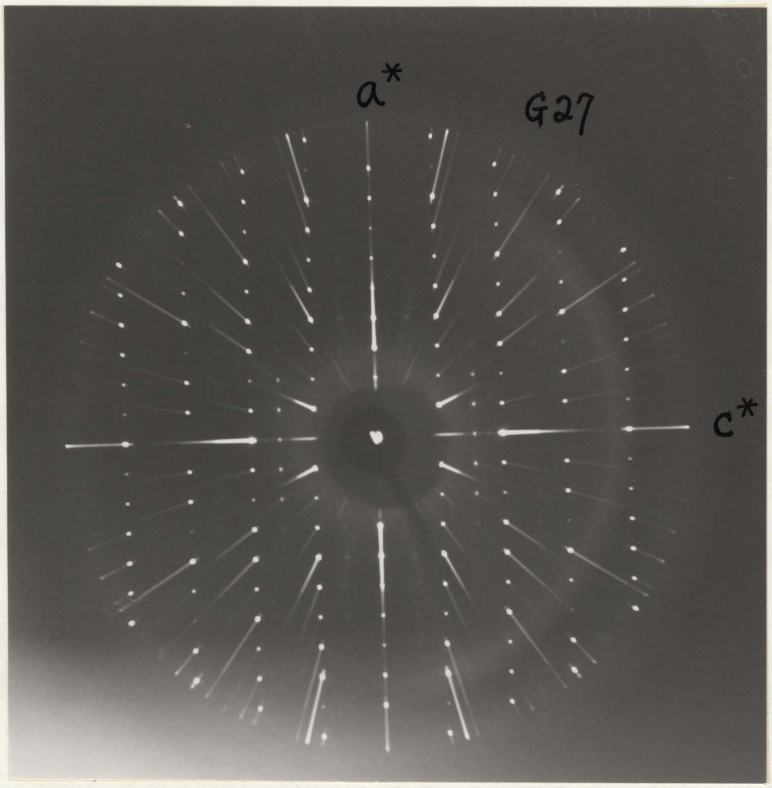

Plate 5 Zero layer of specimen 67001, precessing axis a shows only one set of superstructure reflections. (67001, unheated, MoKα, G27).

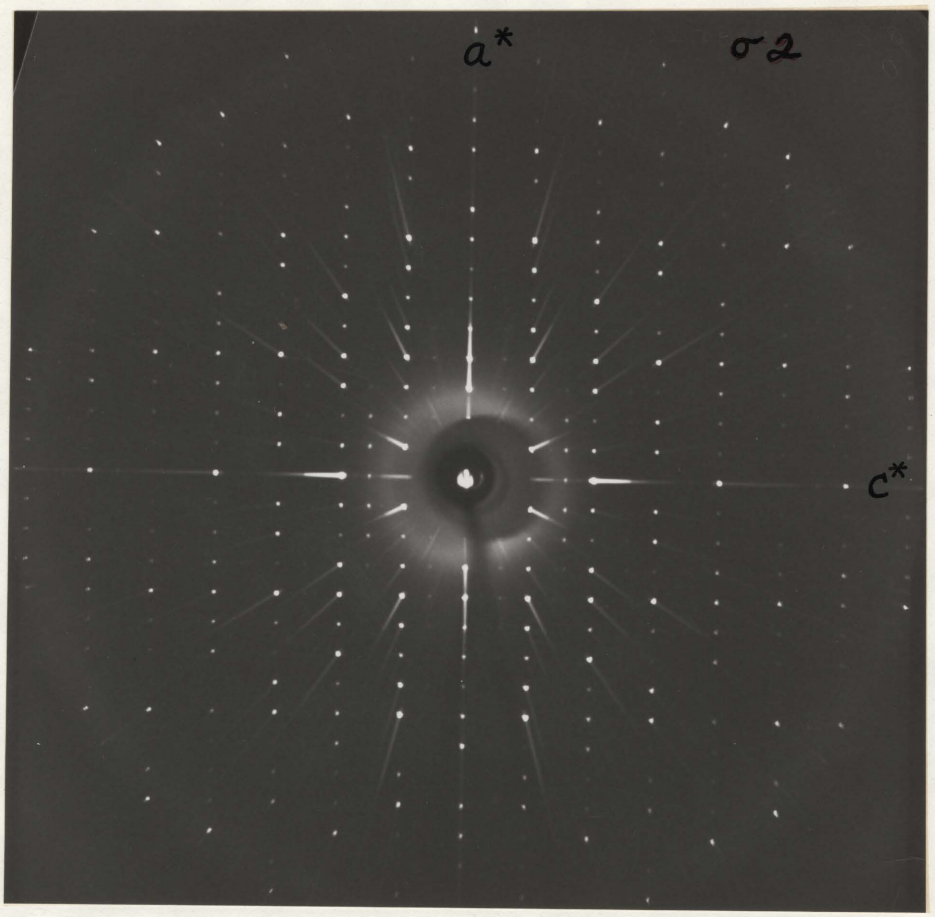

Plate 6 Zero layer of specimen 6900S, precessing axis a shows only one set of superstructure reflections. (6900S, unheated, MoKα,σ2).

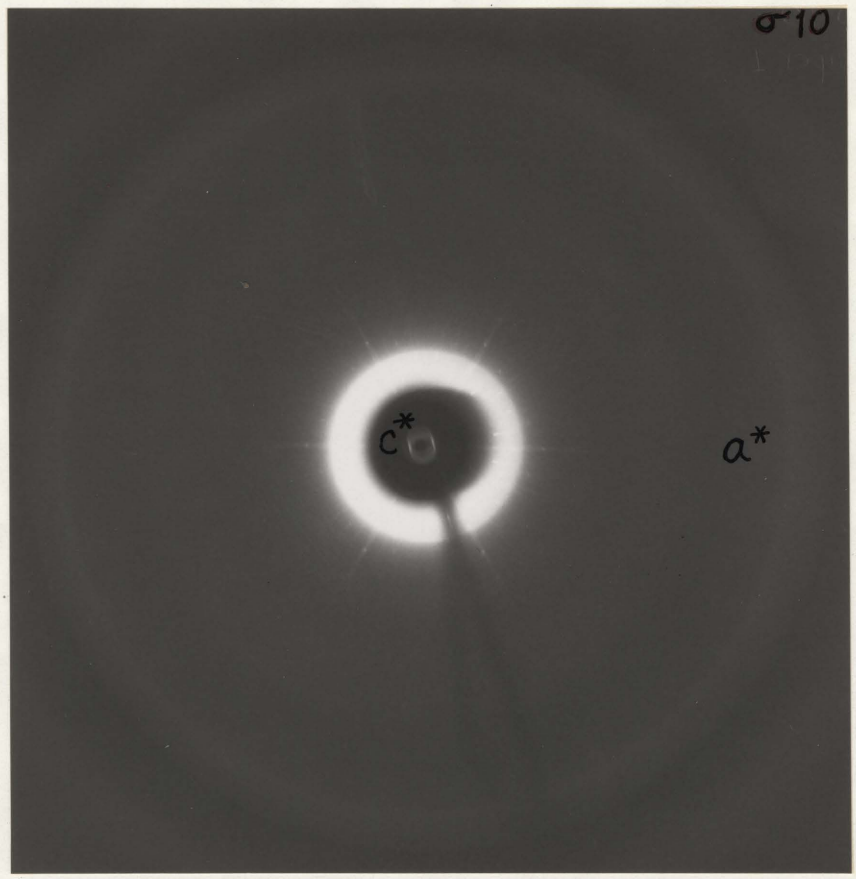

Plate 7 Second layer of superstructure reflections, precessing axis c, shows 6-fold symmetry. (6900S unheated, MoKα,σ10).

All of the studied cancrinites show superstructure reflections which are different from one specimen to another in abundance, position (spacing) and intensities of the reflections. It is worthwhile to mention that a cancrinite found in the skarn of York River, Bancroft, shows remarkably intense superstructure reflections (Peacor, Univ. of Michigan, personal communication).

The possible superstructure reflections were reported by Jarchow (1965) as diffuse satellites with indices ($h\ k\ l \pm \frac{3}{7}$.) Irrational indices can also be assigned to each set of superstructure reflections in Table 2-4 but different from Jarchow's indices.

It is possible that twinning or inclusions in cancrinite will result in the same pattern of reflections as the superstructure reflections. Although cancrinites invariably show non-Bragg reflections which are different from specimen to specimen, there is no definite relation such as a twin law between the non-Bragg reflections and the main lattice reflections, and the intensities of the former are much weaker than the latter. Furthermore, in a heated cancrinite, the non-Bragg reflections decrease in intensities very rapidly with increasing temperatures. This is not the case if it is a twinned crystal.

Very probably, the non-Bragg reflections result from inclusions of sodalite group minerals. The fact that the non-Bragg reflections conform exactly to the symmetry and orientation of the main lattice reflections

would support this theory. Sodalite minerals are very similar or identical to cancrinite in chemical composition and in the basic unit of structure which is the ring of six tetrahedra, but they are different in the type of stacking. The stacking disorder in cancrinite and possible sodalite inclusions will be discussed in Chapter 5.

CHAPTER 3

THERMOGRAVIMETRIC ANALYSIS

3-1 Procedure

The sample used in each run was 100 to 150mg of cancrinite powder. The sample was placed in an alumina crucible which was then placed in a Stanton H T D thermobalance. The crucible and sample were weighed before and after running in the thermobalance. To exclude the absorbed water, the crucible and sample were stored in a 110°C furnace over night before running and were stored in a desiccator after running.

The heating rate was 6°C/min., under one atmosphere pressure of air. In one experiment, the heating program was interrupted in order to maintain a constant temperature for a certain period of time until equilibrium at that temperature seemed to be reached.

Weight changes below 300°C were affected by air drafting and buoyancy effects, so the weight loss below 300°C was not studied.

3-2 Results

Table 3-1 gives the weight loss-temperature data for 68024 and 67001 cancrinites. This data is given in graphical form in Fig. 3-1.

Fig. 3-2 shows the weight loss-time curves of 68024 at 600°C, 750°C and 800°C. Different rates of weight loss are evident.

Table 3-1 Weight loss of cancrinites during heating

Temp ^{o}C	Weight loss in %	
	68024	67001
300°C	0.15	0.28
320	0.18	0.34
340	0.26	0.42
360	0.33	0.46
380	0.36	0.55
400	0.49	0.70
420	0.59	0.79
440	0.67	0.90
460	0.71	1.04
480	0.76	1.23
500	0.83	1.36
520	0.89	1.53
540	1.10	1.77
560	1.25	2.00
580	1.41	2.22
600	1.51	2.40
620	1.72	2.67
640	1.85	3.00
660	2.24	3.29
680	2.65	3.51
700	2.83	3.75
720	2.98	3.89
740	3.13	4.04
760	3.23	4.24
780	3.33	4.45
800	3.46	4.68
820	3.61	4.92
840	3.72	5.24
860	3.82	5.91
880	4.08	6.52
900	4.39	6.72
920	4.85	6.80
940	5.92	6.86
960	7.35	6.97
680	8.40	7.06
1000	8.45	7.10
1020	8.51	7.19
1040	8.56	7.33
1060	8.58	7.51
1080	8.61	7.78

Table 3-2 Weight loss of 68024 cancrinites
(equilibrium assumed)

Temp ^{o}C	Time (hrs)	Wt loss in mg	Wt loss in %
300	4.5	0	0
350	17.25	1.5	1.01%
400	9	2.1	1.42
450	15	3.5	2.36
500	9	4.0	2.70
550	13	4.5	3.04
600	7	4.7	3.17
650	19	5.5	3.71
700	15	6.1	4.12
750	7	6.5	4.39
800	13	7.7	5.20
850	21	12.5	8.44
900	6	12.5	8.44
950	16	13.1	8.85

In Table 3-2, the second column shows the time necessary for the sample to reach equilibrium. The sample size was 148mg. The weight difference before and after running measured by ordinary balance was 13.9 mg which is 9.39%. The weight loss counted from the chart was 13.1 mg, which is 8.85%. The difference is due to some weight loss below $300^{o}C$ and buoyancy effects.

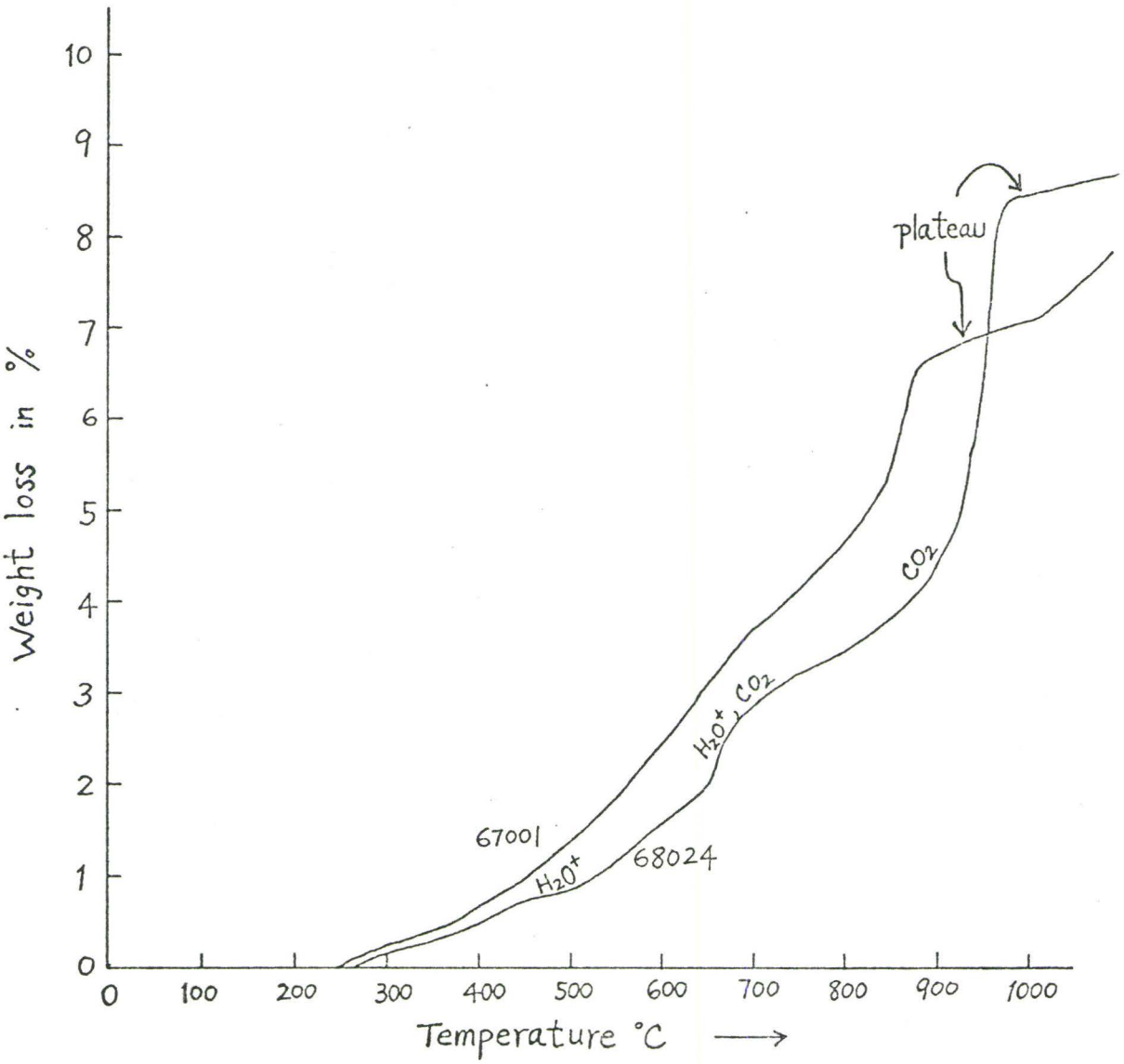

Fig. 3-1 Thermogravimetric curves of 68024 and 67001 cancrinites

Fig. 3-2 The weight loss-time curves of 68024 at 600°C, 750°C and 800°C

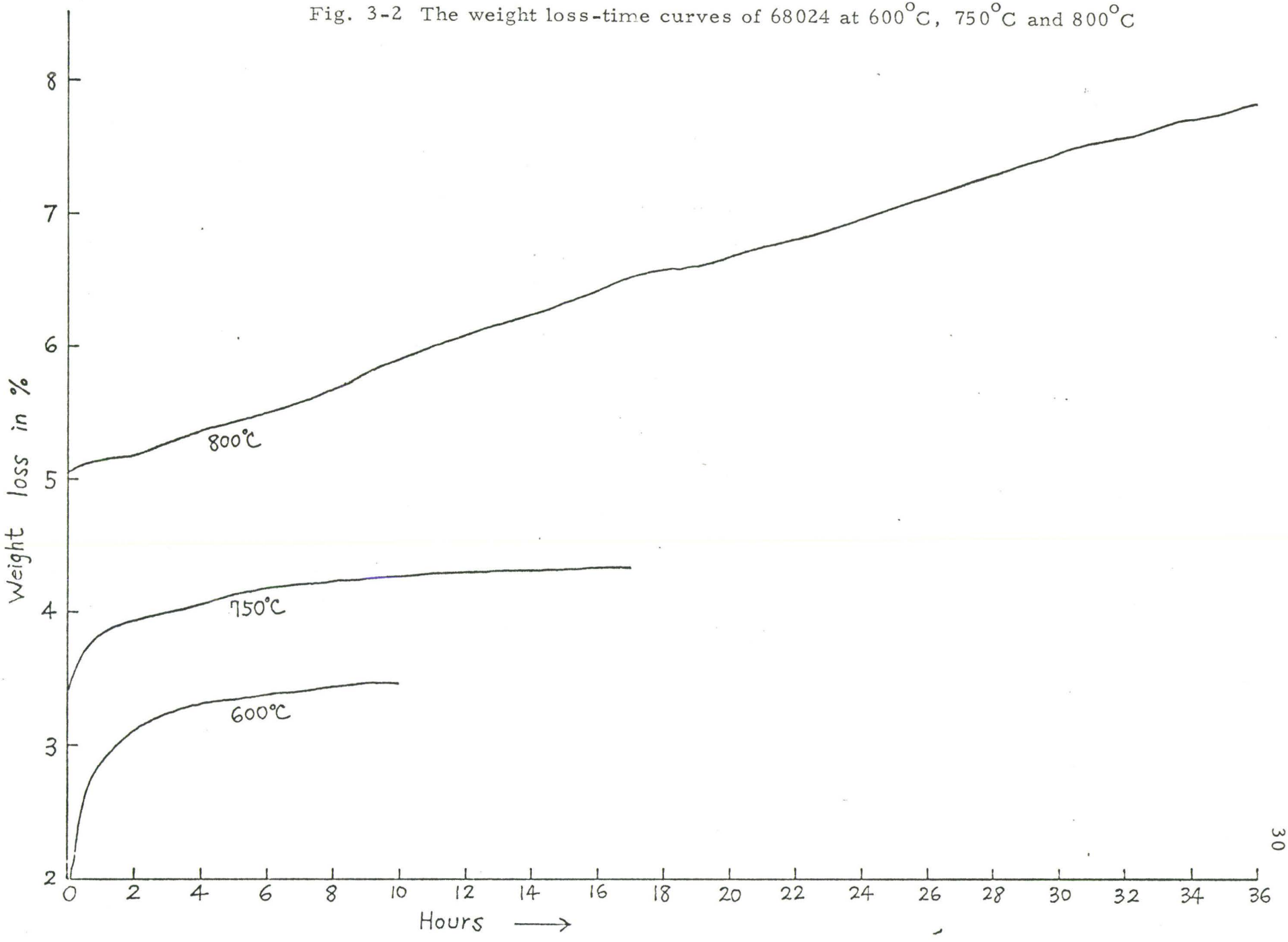

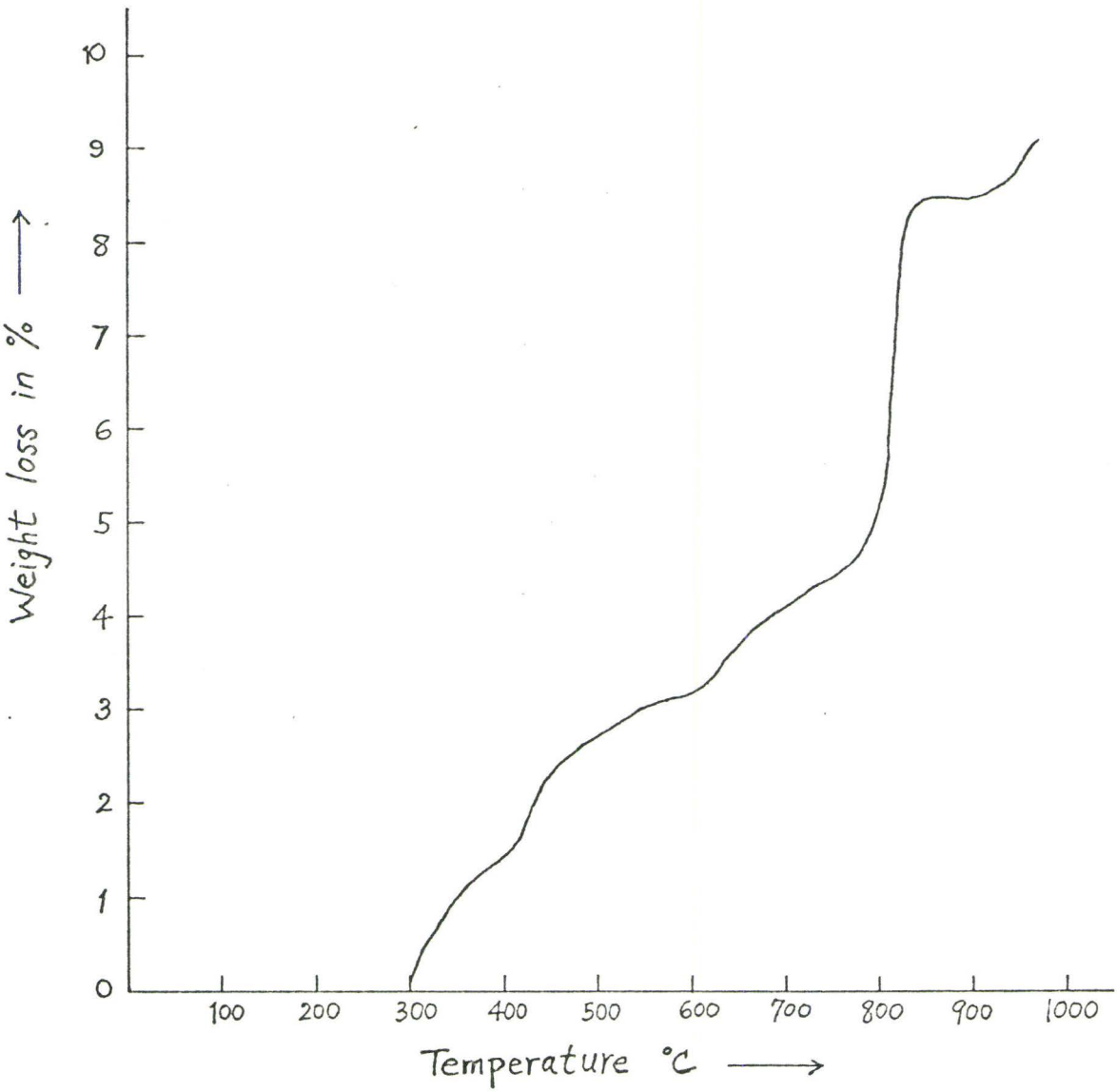

Fig 3-3 Thermogravimetric curve of 68024 (equilibrium assumed)

Table 3-2 gives the thermogravimetric data of 68024, the heating rate was 6°C/min. and was interrupted at 50° intervals until equilibrium appeared to have been reached.

Fig. 3-3 gives the thermogravimetric curve plotted from the data of Table 3-2.

3-3 Discussion

The volatile components in the cancrinite structure, essentially water molecules and CO_2 escape gradually during heating, the general trend of weight loss of specimens 68024 and 67001 is shown in Fig. 3-1. The gases which evolved during heating of the cancrinite powder in the thermobalance were not collected, so that the nature of the gases is not known. It is supposed that H_2O started to evaporate at lower temperatures than CO_2, the CO_2 escaped together with some H_2O at moderately high temperatures. At further high temperatures, H_2O was expelled completely while part of the CO_2 was still in the structure. Accurate temperatures at which the commencement of evaporation of the crystallization -water or of CO_2 can not be obtained by this experiment.

In Fig 3-1, the thermogravimetric curves at 900°C and higher temperatures show a plateau region which corresponds with an endothermic valley of the DTA curve of cancrinite. It is probable that around this temperature region, the cancrinite structure is either decomposed or melted to a liquid state. Comparing the two curves in Fig. 3-1, it is seen that the plateau region of 68024 is 100°C higher than that of 67001. Also the 68024

cancrinite appears more stable but decomposes suddenly while the 67001 cancrinite decomposes gradually at lower temperatures. The differences in the thermogravimetric behavior must be attributed to the differences in chemical compositions which were given in Table 2-1 and Table 2-2.

Consider the volatile components first, 68024 is lower in H_2O and higher in CO_2 content than 67001. Because water of crystallization starts to evaporate at lower temperatures than CO_2, therefore in the low temperature part of the thermogravimetric curves, 68024 has a smaller weight loss and the curve is less steep than 67001, and in the high temperature part, 68024 has much more weight loss than 67001. As to why 68024 is more stable than 67001 at high temperatures, it may be explained by the suggestions made by Kôzu, et al (1933). According to these authors the CO_3^{--} group in the cancrinite structure is bonded in one case to "Na" and in the other case to "Ca". The CO_2 in the former case is expelled at about $100^{\circ}C$ lower temperature than the CO_2 in the latter case when the cancrinite is being heated. Chemical analysis shows 68024 has much higher calcium content than 67001 while the sodium content is the same. This may be why there is large amounts of weight loss in 68024 at high temperatures. The high potassium content in 67001 also affects its stability compared to 68024 at high temperatures.

Because the volatile components escape gradually during heating and a relatively high heating rate was used, equilibrium at each temperature was

not reached. Comparing Fig. 3-3 to Fig. 3-1, the general shape of the curves is the same but the temperature readings of the equilibrium curve are about 130 ^{o}C lower than the readings taken from the non-equilibrium curve. For example, the large weight loss occurred between 800^{o}C to 850^{o}C in the equilibrium curve, and between 920^{o}C to 980^{o}C in the non-equilibrium curve of 68024.

The heating experiments based on the results of the equilibrium thermogravimetric curve are discussed in the next chapter.

CHAPTER 4

HEATING EXPERIMENTS

4-1 Method

In order to determine if there is any change in the cell dimensions and the non-Bragg reflections after heating, some cancrinite powder and single crystals were heated in a furnace. Samples of specimens 68024, 67001, 67002 and 6900S were sealed closed in gold capsules, then placed on the end of a thermocouple and inserted in a furnace. In this way, the temperature was maintained to within $\pm 5^{\circ}C$.

The heating experiments were done at $600^{\circ}C$, $745^{\circ}C$ and $800^{\circ}C$ respectively, each heating lasted for 8 days. Then precession photographs were taken of the single crystals and the powders were run on an x-ray diffractometer after the specimens were quenched to room temperature. In the heating experiments, only irreversible changes can be detected.

4-2 Studies on powder diffraction patterns

(i) Refinement of unit cell dimensions

The cancrinite powder was ground and mixed in the proportion of 4 : 1 with very pure quartz from Oliver, B.C. The latter was used as an internal standard. The prepared sample was then examined with an x-Ray diffractometer using $CuK\alpha$ monochromatic radiation from a high intensity copper tube. A complete powder diffraction pattern from 6° to $125^{\circ} 2\theta$ was run. The slits and scales were subjected to change at high angles.

The position of all the quartz peaks in the pattern was determined with a centimeter scale. Then a curve was drawn relating this measurement to the known 2θ positions of the quartz peaks. This graphical relationship holds for all peaks on the same chart. So all the 2θ measurements of the cancrinite peaks can be obtained if their positions on the chart are measured.

Some intense peaks of cancrinite were indexed, and then run through a CDC 6400 computer using a least squares program to calculate the appropriate cell dimensions. At the same time, a list of all possible indices and "d" spacings was generated. More indexed cancrinite peaks were selected from the diffraction pattern to run through the least squares program and another set of cell dimensions was calculated. The above procedure was repeated several times until all the cancrinite peaks were used. Reasonably accurate cell dimensions were obtained in this manner. The precision is within $\pm$. 003 Å.

Table 4-1 is a list of cell dimensions calculated for specimens 68024, 67001, 67002 and 6900S compared to cell dimensions of cancrinite from other localities.

The calculated cell dimensions of the Ontario cancrinites 68024, 67001, 67002 and 6900S agree closely to within 0.05%. They are similar to the cell dimensions obtained from single crystal studies by Phoenix and Nuffield (1949) and from the powder method for the New Hampshire specimen by Edgar.

Table 4-1 A list of cell dimensions of cancrinite from different localities

Locality	Author	a_o (Å)	c_o (Å)
Monte Somma, Vesuvius	Zambonini & Ferrari (1930)	12.73	5.10
Miask, Urals	Gossner & Mussgnug (1930)	12.60	5.18
Dôdô, Korea	Kôzu & Takane (1933)	12.72	5.18
Monte Somma (Davyne)	Gossner & Mussgnug (1930)	12.80	5.35
Blue Mountain, Ontario	Phoenix & Nuffield (1949)	12.60	5.12
Litchfield, Maine	Nithollon (1955)	12.56	5.09
Red Hill, New Hampshire	Edgar (1964) lemon yellow	12.60	5.12
Methuen Tp. Ontario	Edgar (1949) yellow	12.60	5.14
Methuen Tp. Ontario	Edgar (1964) purplish pink		
Loch Borolan, Scotland	Edgar (1964) sulphatic	12.68	5.18
Litchfield, Maine	Jarchow (1965)	12.75	5.14
Dungannon Tp. Ontario	68024 pinkish white	12.616	5.125
Methuen Tp. Ontario	67001 yellow	12.615	5.125
Dungannon Tp. Ontario	67002 white	12.617	5.125
Methuen Tp. Ontario	6900S yellow	12.611	5.124

Table 4-2 Cell dimensions of heated cancrinites

specimen / cell dimension / temperature	68024 a_o(Å)	68024 c_o(Å)	68024 cell volume(Å^3)	67001 a_o(Å)	67001 c_o(Å)	67001 cell volume(Å^3)
unheated	12.616	5.125	706.44	12.615	5.125	706.25
600°C	12.605	5.113	703.65	12.604	5.113	703.34
745°C	12.610	5.108	703.38	12.601	5.111	702.77
800°C	12.600	5.110	702.64	——	——	——

In general, the cell dimensions and the cell volumes of heated cancrinites decrease slightly with heated temperatures. The change of a_o is within 0.15%, c_o within 0.35% and cell volume within 0.60%. New phases having a nepheline and nosean structure appear in all the heated cancrinites between 700°C and 800°C. The cancrinite phase itself disappeared completely in specimen 67001 heated to 800°C. A complete description of phase changes will be given in the following section.

(ii) Phase changes

When the heated cancrinite powders were run on an x-ray diffractometer, phase changes have been detected. Between 700°C and 800°C, two new phases appear to coexist with cancrinite phase, one has a nepheline structure, the other has a sodalite structure. After complete break down of the cancrinite structure, sodalite minerals associate with a nepheline phase. At around 900°C, only a nepheline phase occurs in the residue.

The two specimens, 67001 and 6900S which are honey-yellow in colour, decomposed to nepheline and nosean at temperatures below 745°C. The two white specimens, 68024 and 67002 decomposed between 745°C and 800°C to nepheline and sodalite. In general, the yellow cancrinite decomposed at lower temperatures than the white cancrinite, both changed to nepheline and sodalite group of minerals.

The nepheline phase occurred in specimen 67002 below 745°C while no nepheline phase was observed at 745°C in specimen 68024. Powder of specimen 68024 was heated to 900°C in the thermobalance, and only the nepheline phase survived. It is probable that the nepheline structure was formed at lower temperatures and persisted to higher temperatures than sodalite minerals.

Table 4-3 gives the phase changes in heated cancrinites. In the break down products of 68024 and 67002 cancrinites, the sodalite phase was not easily observed in the powder diffraction pattern, since most of the strong sodalite peaks coincide with the cancrinite peaks, See Table 4-7.

Table 4-3 The phase changes in heated cancrinites

Specimen	Colour	600°C	745°C	800°C	900°C
68024	pinkish white	cancrinite	cancrinite	cancrinite nepheline sodalite	nepheline
67001	honey yellow	cancrinite	cancrinite nepheline nosean	nepheline nosean	
67002	white	cancrinite	cancrinite nepheline	cancrinite nepheline sodalite	
6900S	honey yellow	cancrinite	cancrinite nepheline nosean	nepheline nosean	

Although some of the sodalite peaks can not be separated from the cancrinite peaks, the sodalite phase was identified in the following ways:

1. Comparison of the relative height of cancrinite peaks in the powder diffraction chart of a heated specimen. For example, the cancrinite (211) reflection is supposed to be the strongest reflection and the (211) peak should be the highest of all cancrinite peaks. But in the 67002 800°C specimen, the cancrinite (030) peak is higher than cancrinite (211) peak. In this case, it is possible that the reflections of other phases superimpose upon the cancrinite (030) reflection. It was found that sodalite (211) reflection, which is the strongest reflection of sodalite, has the same 2θ reading and d spacing as cancrinite (030).

2. It was assumed that the cancrinite peaks of 745°C specimen, as a whole, were higher than the cancrinite peaks of 800°C specimen, since in the latter case, there were more nepheline and sodalite formed. The more new phases formed, the more cancrinite decomposed.

3. There was a peak at 31.53° 2θ which could not be indexed either as cancrinite peak or nepheline peak or nosean peak. The reflection must be due to a new phase other than these three, and it can be indexed as sodalite (310).

4. According to Taylor, sodalite and hauyne have the same space group $P\bar{4}3n$, while the space group of nosean is $P\bar{4}3m$. In a powder diffraction pattern, nosean can be distinguished from sodalite and hauyne by the presence of a (100) reflection. Sodalite is different from hauyne

and nosean in that sodalite has a smaller cell dimension than the other two.

Probably there was a small amount of a sodalite phase present in 68024 and 67002 specimens heated to 745°C. It could not be proved because the sodalite reflections were not strong enough to greatly affect the height of the cancrinite peaks.

The calculated cell dimensions of the new formed nepheline, nosean and sodalite are given in Table 4-4. Indices, d spacing and 2θ of the nepheline, nosean and sodalite are listed in Table 4-5, 4-6 and 4-7.

The change of cancrinite to nepheline and cancrinite to sodalite minerals are confirmed in the heating experiments. The crystallographic orientational relation between cancrinite and nosean has been worked out by Van Peteghem and Burley (1962) and Edgar and Burley (1963). They showed that if the c-axis of the hexagonal cancrinite was placed parallel to the [111] axis of the cubic nosean and the a-axis of cancrinite placed parallel to $[0\bar{1}\,1]$ axis of the cube, the resulting cells have the same dimensions as nosean.

This relationship holds for cancrinite → sodalite reaction. The crystallographic orientation of nepheline with respect to cancrinite has not been established. It is questionable whether the cancrinite → nepheline reaction proceeds in a crystallographically ordered manner. Consider the calculated cell dimensions of nepheline and cancrinite, simple numerical relations seem to exist. If the a dimension of cancrinite is taken as 12.615 Å, then two times this dimension will be 25.23Å. If this value is divided by 3, 8.41 Å, the c dimension of nepheline is almost obtained.

Table 4 - 4 The calculated cell dimensions of the new formed nepheline, nosean and sodalite

Specimen	Nepheline a_o (Å)	Nepheline c_o (Å)	Nosean a_o (Å)	Sodalite a_o (Å)
67001 745°C	9.970	8.345	9.021	——
67001 800°C	9.967	8.345	9.028	——
68024 800°C	9.971	8.353	——	8.900

Table 4-5 Nepheline

Indices hkl	67001 (745°C)		67001 (800°C)		68024 (800°C)	
	d (Å)	°2θ(CuKα)	d (Å)	°2θ(CuKα)	d (Å)	°2θ(CuKα)
002	4.176	21.282	4.178	21.267	4.169	21.311
201	3.833	23.199	3.835	23.190	3.837	23.174
120	3.262	27.329	3.264	27.320	3.262	27.338
202	3.001	29.760	3.001	29.762	3.001	29.760
122			2.569	34.912		
203	2.338	38.473(α1)	2.338	38.468(α1)	2.340	38.429(α1)
131			2.301	39.127(α1)		
004			2.086	43.337(α1)		
205			1.557	59.299(α1)		
333			1.426	65.367(α1)		
520			1.382	67.748(α1)		
325			1.276	74.262(α1)		
443			1.137	85.289(α1)		
525			1.065	92.711(α1)		
156			1.035	96.152(α1)		
327			1.022	97.890(α1)		
724			0.941	109.876(α1)		

Table 4-6 Nosean

Indices hkl	67001 (745°C)		67001 (800°C)	
	d(Å)	°2θ(CuKα)	d(Å)	°2θ(CuKα)
100	9.027	9.803	9.006	9.815
110	6.382	13.872	6.376	13.881
111			5.212	17.007
211	3.687	24.148	3.688	24.134
310	2.857	31.298	2.858	31.291
222	2.608	34.389	2.608	34.382
321			2.412	37.254(α1)
400			2.258	39.886(α1)
401			2.191	41.174(α1)
411	2.126	42.489(α1)	2.127	42.474(α1)
313			2.071	43.667(α1)
332			1.925	47.188(α1)
510	1.768	51.650(α1)	1.771	51.578(α1)
521			1.648	55.718(α1)
440	1.595	57.767(α1)	1.595	57.751(α1)
035			1.549	59.648(α1)
006			1.504	61.601(α1)
116			1.464	63.464(α1)
226			1.361	68.913(α1)
444			1.303	72.489(α1)
217			1.229	77.638(α1)
800			1.129	86.088(α1)

Table 4 - 7 Sodalite

Indices hkl	68024 (800°C)		Indexed as cancrinite
	d (Å)	°2θ (CuKα)	
110	6.298	14.070	110
211	3.636	24.482	030
310	2.837	31.533	——
222	2.559	35.054	002
330	2.093	43.193(α1)	330
440	1.575	58.564(α1)	440

Furthermore, twice the c dimension of cancrinite, 10.25 Å, gives almost the a dimension of nepheline. The following shows these calculations:

Cancrinite	Nosean	Sodalite	Nepheline
a_o = 12.615 Å	a_o = 9.02	a_o = 8.90	a_o = 9.97
c_o = 5.125 Å	V = 734	V = 705	c_o = 8.35
V = 706 Å^3			V = 718

$a_{cancr}(12.615) \simeq \sqrt{2}x\ a_{nosean}(12.75)$ (1% expansion)

$3x\ c_{cancr}(15.375) \simeq \sqrt{3}x\ a_{nosean}(15.64)$ (1.7% expansion)

$V_{cancr}(706) \simeq V_{nosean}(734)$ (4% expansion)

$2x a_{cancr}(25.23) \simeq 3x\ c_{neph}(25.05)$ (0.7% contraction)

$2x c_{cancr}(10.25) \simeq a_{neph}(9.97)$ (2.7% contraction)

$V_{cancr}(706) \simeq V_{neph}(718)$ (1.7% expansion)

4-3 Studies on the heated single crystals of cancrinite

(i) Change in superstructure

The superstructure reflections in the unheated crystals of cancrinite were described in detail in Chapter 2, section 2-5. It was mentioned that there were one to three sets of superstructure reflections, and the "f" set was the most intense one. If one examines the precession photographs of 68024 cancrinite heated to 410°C (Plate 8), it may be seen that the intensities of the superstructure reflections decrease so much that the "d" and "e" sets disappear completely and the "f" set appears as very light linear traces, only the most intense reflections between (0kl) and (0k2) of the main lattice reflections can be easily seen. In the 68024 600°C specimen (Plate 9), the intensities of the most intense reflections between (0kl) and (0k2) reflections decrease slightly compared to the 410°C specimen.

In 68024 745°C photograph (Plate 10), the superstructure reflections between (0kl) and (0k2) are very weak and almost disappear. Heating experiments up to 800°C on specimen 68024 resulted in very poor photographs which were not decipherable.

For unheated specimen of 67001, only an "f" set of superstructure reflections is present, whose intensities decrease greatly in the specimen heated to 600°C, linear traces of the most intense reflections between (0kl) and (0k2) are present, (Plate 11). At 745°C, superstructure reflections disappear completely and reflections of new phases occur, (Plate 12).

Besides decreasing in intensities, the position of the superstructure reflections in the $a^* c^*$ reciprocal lattice plane varies with temperatures. In general, the linear traces which are always parallel to the a^* - axis and perpendicular to the c^* - axis shift towards the origin. The distance of shifting varies with specimens and temperatures, 68024 and 67001 behave very similarly to 67002 and 6900S respectively. From Table 4-8, it may be seen that superstructure reflections shift with an increase in temperature, in other words, the superstructure spacing perpendicular to c- axis increases with temperature increasing. The ratio of superstructure spacing to d_{001} spacing of the main structure varies between 1.54 to 2.09 in the four specimens.

In the heated specimens, the superstructure reflections are streaked lines parallel to the a^* - axis, rather than lines of spots as in unheated

Table 4-8 Ratio of superstructure spacing to d_{001} spacing of the main lattice at different temperatures

specimens / temperatures	68024		67001		67002		6900S	
	position of "f"	ratio to d_{001}	position of "f"	ratio to d_{001}	position of "f"	ratio to d_{001}	position of "f"	ratio to d_{001}
unheated	5.25mm	1.58	4.61mm	1.80	5.36mm	1.54	4.68mm	1.79
600°C	4.81mm	1.73	3.99mm	2.09	4.84mm	1.72	4.16mm	2.00
745°C	4.40mm	1.94			4.38mm	1.91		

specimens. This means some kind of disordering occurs in the plane perpendicular to the c^* - axis and the d_{100} spacing of the superstructure varies. Unlike unheated specimens, the superstructure has the same d_{100} spacing as the main structure.

(ii) Reflections from new phases in precession photographs of cancrinite

In specimen 68024 heated to 410°C and 600°C, a few reflections from a new phase appeared on the precession photographs, (see Plate 8 and 13). These reflections appear to be from a sodalite mineral.

In the precession photographs of specimen 67001 heated to 745°C, a number of new reflections appeared in addition to the cancrinite reflections, indicating phase changes had occurred. From powder diffraction data of 67001 heated to 745°C it was seen that cancrinite coexisted with two new phases, nepheline and nosean. In the single crystal photograph, the well-oriented nosean and nepheline patterns of spots develop while the cancrinite pattern of spots is still visible. (see Plate 14).

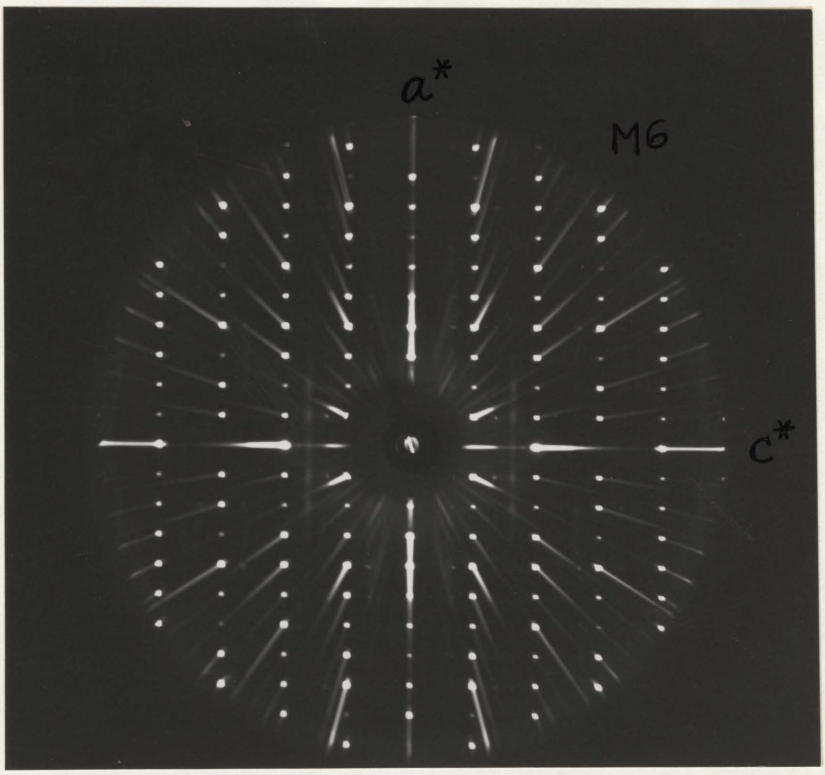

Plate 8 Zero layer of specimen 68024 heated to 410°C. Notice that the superstructure reflections are streaked, "d" and "e" sets disappear completely. (68024, 410°C, MoKα, M6).

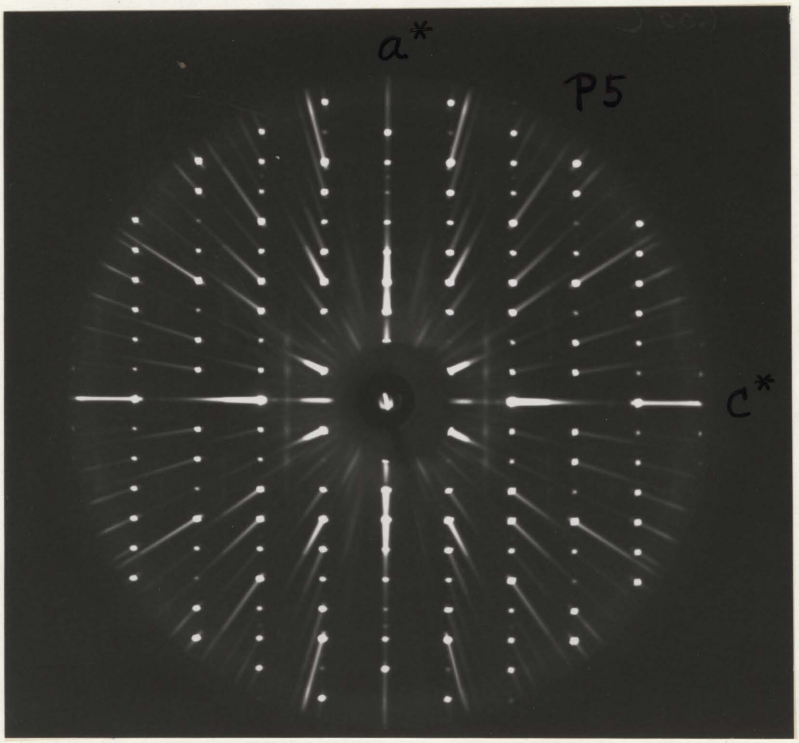

Plate 9 Zero layer of specimen 68024 heated to 600°C. Notice that the intensities of the superstructure reflections decrease slightly compared with Plate 8 (68024, 600°C, MoKα, P5).

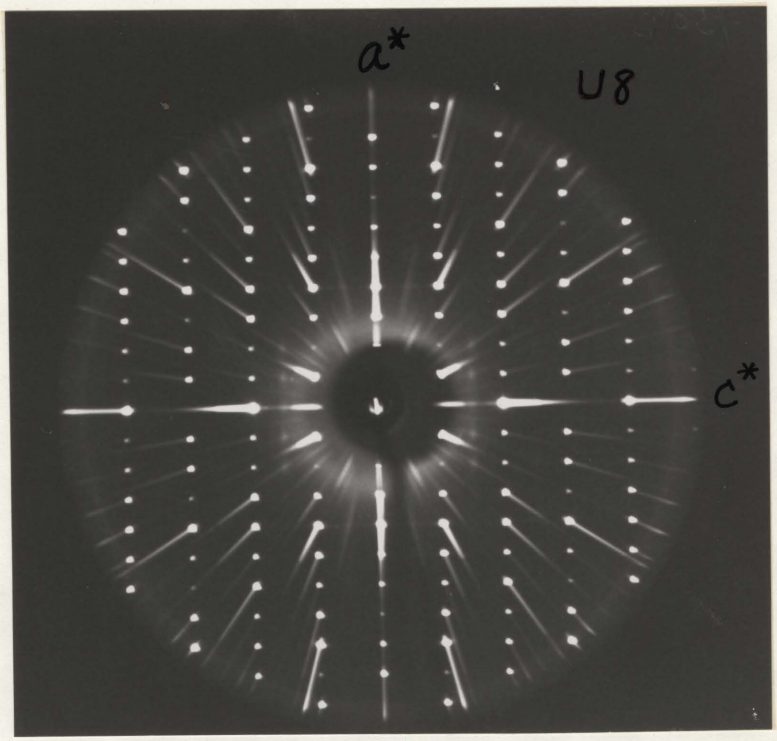

Plate 10 Zero layer of specimen 68024 heated to 745°C. The superstructure reflections are very weak and almost disappear (68024, 745°C, MoKα, U8).

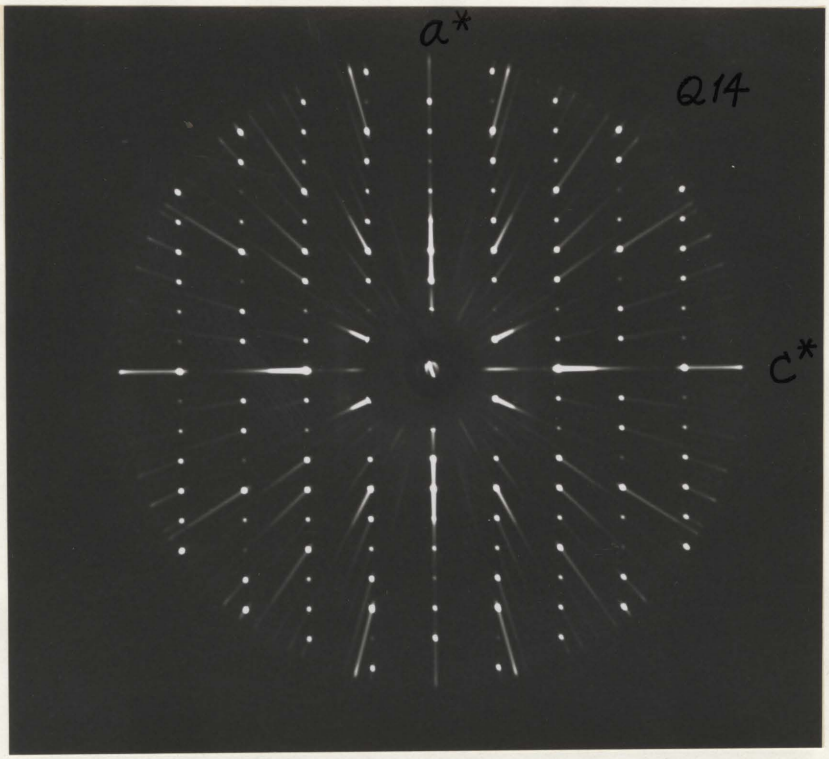

Plate 11 Zero layer of specimen 67001 heated to 600°C. Notice the very weak intensities of the superstructure reflections. (67001, 600°C, MoKα, Q14).

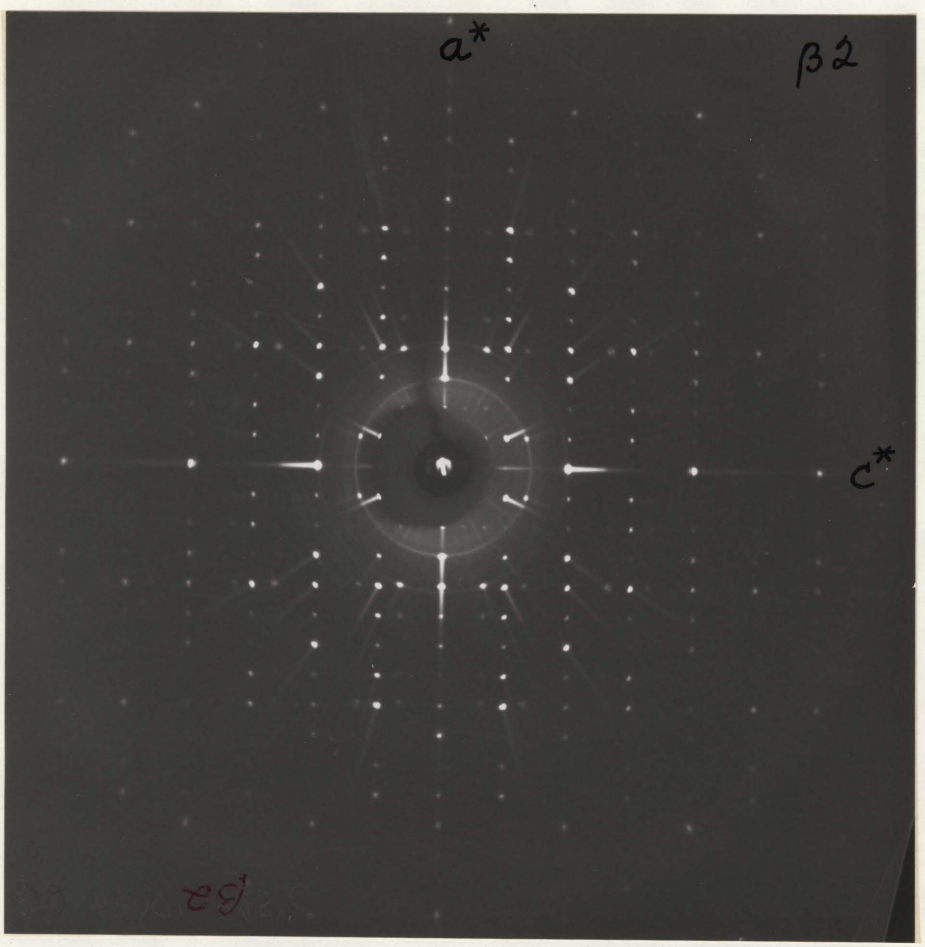

Plate 12 Zero layer of specimen 67001 heated to 745°C. Notice the complete disappearance of superstructure reflections and reflections of new phases occur. (67001, 745°C, MoKα, β 2).

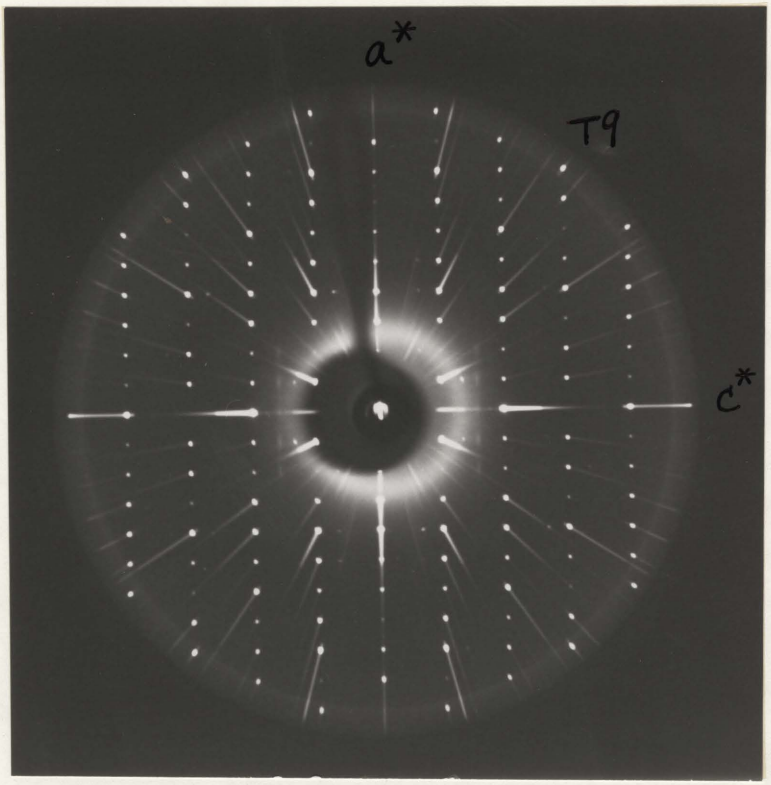

Plate 13 Zero layer of specimen 68024 heated to 600°C. New reflections which appear to be from a sodalite mineral occur. (68024, 600°C, MoKα , T9).

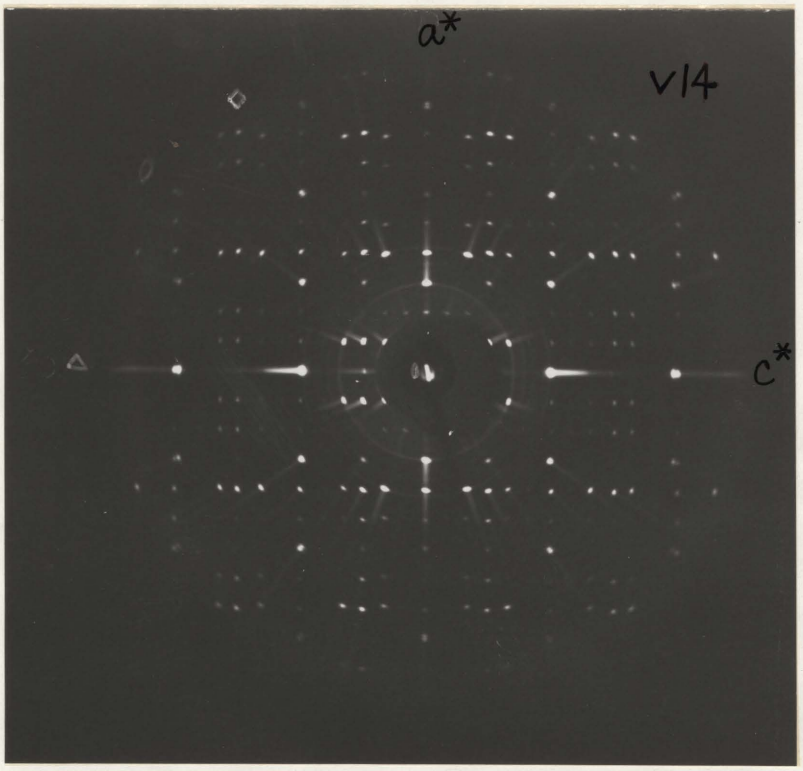

Plate 14 Zero layer of specimen 67001 heated to 745°C. The well-oriented nosean and nepheline reflections develop while the cancrinite reflections are still visible. (67001, 745°C, MoKα, V14).

CHAPTER 5

DISCUSSION AND CONCLUSION

5-1 Superstructure reflections

Specimens 68024 and 67002 are more abundant in superstructure reflections than specimens 67001 and 6900S. The former specimens are pinkish white or white in colour, from Dungannon Township, Ontario. The latter specimens are honey-yellow, from Methuen Township, Ontario. It was found that the cancrinite from skarn of York River, Bancroft shows very intense superstructure reflections.

All of the superstructure reflections have the same symmetry elements and systematic extinctions as the main lattice reflections, but the intensities, abundances and the relative positions with respect to the main lattice reflections are different from one specimen to another. The systematic extinction of the superstructure reflections was identified by the absence of an a^*-axis streak on possible superstructure reflection between the (002) and (003) reflections of the main lattice. See Plate 8, specimen of 68024 heated to 410°C. It is very probable that the superstructure reflections are affected by chemical environment, pressure and temperature conditions when a cancrinite is formed. To determine the relative importance of these three factors requires a great deal of chemical

analysis data and single crystal photographs of cancrinite from different localities. The variability of the superstructure reflections may indicate the chemical and physical conditions in which a cancrinite was formed.

In the heated specimens, the superstructure reflections decrease in intensities, shifts in position. In addition, they are streaked in a direction parallel to the a^*-axis on the $a^* c^*$ reciprocal lattice plane.
The changes of the superstructure reflections after heating provides evidence as to the origin of the superstructure reflections. Two probable origins may be suggested for the superstructure reflections of cancrinite.

(i) Stacking disorder of the ring of six tetrahedra which is the basic stacking unit of cancrinite, sodalite and other silicates. Cancrinite is in ABABA... stacking and sodalite group minerals are in ABCABCAB... stacking. Stacking faults in cancrinite may occur in two ways (1) A layer is not followed by B layer or vice versa. (2) B layer is not followed by A layer but followed by C layer, and then a mineral structure like sodalite occurs. If this kind of stacking fault occurs very often, the sodalite may be treated as an inclusion in cancrinite.

(ii) A disorder of individual cation, anion group or water molecule within the frame work of cancrinite.

If the stacking faults of the misplaced anion groups represent disequilibrium, then by heating the cancrinites, the true equilibrium configuration

may be reached, and in this case the intensities of the non-Bragg reflections will decrease.

A disordering of the superstructure in a plane perpendicular to c^* - axis will result in a streaked superstructure reflection parallel to the a^* - axis. Either disordering in the arrangement of volatile components or disordering of the hexagonal rings will make the streaked reflections possible.

The sodalite group of minerals have the same subcell as cancrinite hexagonal rings of (Al, Si) O_4 tetrahedra. These two minerals may be polymorphic, or polytypes as in mica. Therefore, the superstructure in cancrinite might also be treated as a phase between the cancrinite and sodalite group of minerals.

5-2 Phase changes

In the heating experiments, the cancrinite was heated in a dry condition and open system, reaction rates were very slow, metastable phases and transitional phases may occur. In the reactions, cancrinite to sodalite and nepheline or cancrinite to nosean and nepheline, sodalite and nosean occur as transitional phases, nepheline is a stable phase or end product of the heating of cancrinite under these conditions.

The transformation model of cancrinite to sodalite or nosean is not known, except the crystallographic orientational relation. The thrust of a whole hexagonal ring of (Al, Si) O_4 tetrahedra from ABAB$\cdots$ stacking of cancrinite to ABCABC$\cdots$ stacking of sodalite or nosean is energetically

difficult because it breaks many bonds in the (001) plane of cancrinite which is not a cleavage plane.

According to Pauling's framework of cancrinite structure, the 6-fold screw axis falls at the centre of the big channels, and the 3-fold axis falls at the centre of hexagonal rings which are in a plane perpendicular to the c-axis. It is easier to break every other bond in some of the hexagonal rings of cancrinite and form some new hexagonal rings on top and bottom of the big channels in the cancrinite framework. In this way the big channels are enclosed, and the holes around the 3-fold axis of cancrinite framework are expanded to the volume of the holes in the sodalite framework.

Different specimens of cancrinite transformed to nosean and nepheline or sodalite or nepheline during heating. This may be attributed to the difference in chemical compositions of cancrinite specimens.

5-3 Conclusions

The occurrence of non-Bragg reflections in cancrinite is still a problem. Do the non-Bragg reflections occur because of superstructure in cancrinite? If so, what is the origin of the superstructure and what kind of superstructure is it? To answer these questions, we need more cancrinite specimens with various compositions from different localities. It is certain that the non-Bragg reflections are something very similar to the main lattice reflections and their intensities decrease with in-

creasing temperature. There may be some kind of relation between the non-Bragg reflections in cancrinite and the sodalite group of minerals.

How a cancrinite structure transforms to a sodalite structure is not known, but a rough idea is suggested. The cancrinite to nepheline reaction may proceed in a crystallographically ordered manner as shown in Plate 14.

REFERENCES

BELIANKIN, D. S. (1944), Vishnevite, and not Sulphatic Cancrinite Compt. Rend (Doklady) Acad. Sci., URSS 42:304-306.

BORDNER, J. and GORDON, L. (1962), Thermogravimetry of some Uranium^{VI} 8-Hydroxyquinolates. Talanta 9:1003-1007.

BRINDLEY, G. W. (1963), Crystallographic Aspects of Some Decompostion and Recrystallization Reactions. Progress in Ceramic Science 3 MacMillan, New York.

BUERGER, M. J. (1964), The Precession Method in X-Ray Crystallography John Wiley & Sons, Inc. 1964.

_____, (1966), X-Ray Crystallography, 7th printing John Wiley & Sons, Inc.

DEER, W. A., HOWIE, R. A. and ZUSSMAN, J. (1966), An Introduction To The Rock-Forming Minerals. Longmans, Green and Co. Ltd.,

EDGAR, A. D. and BURLEY, B. J. (1963), Studies on Cancrinites. I— Ploymorphism in Sodium Carbonate Rich Cancrinite - Natrodavyne Canadian Min., 7:631-642.

EDGAR, A. D. (1964), Studies on Cancrinites, II—Stability Fields and Cell Dimensions of Calcium and Potassium - Rich Cancrinites. Canadian Min., 8:53-67

EITEL, W., (1922), Über das System $CaCO_3$-$NaAlSiO_4$ (Calcit - Nephelin) und den Cancrinite. N. Jb. Min. 1922, II:45-61.

LONSDALE, K. (1965), International Tables for X-Ray Crystallogarphy I The Kynoch Press, Birmingham, England.

JARCHOW, O. (1965), Atomanordnung und Strukturverfeinerung von Cancrinit. Zeit Kristallogr. Bd. 122, S. 407-422.

_____, (1963), Die Strukturbestimmung des Cancrinits. Acta Crystallogr., Rome Abstract 2.4.

KÔZU, S., SETO, K. and TSURUMI, S. (1932), Chemical Composition of Cancrinite from Dôdô, Korea. Proc. Imp. Acad. Tokyo, 8:432-435.

KÔZU, S. and TAKANÉ, K. (1933), Crystal Structure of Cancrinite from Dôdô, Korea. Proc. Imp. Acad. Tokyo, 9:56-59, 105-108.

KÔZU, S. UEDA, J. and TSURUMI, S. (1933) Optical and Thermal Properties of Cancrinite from Dôdô, Korea. Proc. Imp. Acad. Tokyo, 9:13-16.

NITHOLLON, P. (1955), Structure Cristalline de la Cancrinite. Publications Scientifiques et Techniques du Ministére de láir France, N. T. 53.:48

PAULING, L. (1930), The Structure of Some Sodium and Calcium Aluminosilicates. Proc. Nat. Acad. Sci. 16:453-459.

PHOENIX, R. and NUFFIELD, E. W. (1949), Cancrinites from Blue Mountain, Ontario. Amer. Min., 34:452-455

SMITH, J. V. and YODER, H. S. (1956), Experimental and Theoretical Studies of the Mica Polymorphs. Min. Mag. 31 :209

TAYLOR, D. (1967), The Sodalite Group of Minerals. Contr. Mineral and Petrol 16:172-188.

VAN PETEGHEM, J. and BURLEY, B. J. (1962), Studies on the Sodalite Group of Minerals. Trans. Roy. Soc. Canada, LVI Ser. III Sect. III, p. 37-53.